

Exact Critical Behavior of Two-Dimensional Wetting Problems with Quenched Disorder

G. Forgacs,¹ J. M. Luck,² Th. M. Nieuwenhuizen,³ and H. Orland^{2,4}

Received September 22, 1987; revision received December 18, 1987

The wetting transition in the presence of a random substrate is studied in two dimensions, using a restricted solid-on-solid model. The singular part of the quenched free energy and specific heat is calculated exactly by means of the replica trick. Disorder introduces logarithmic corrections to the results of the pure system. The divergent part of the width of the wetting layer is also evaluated: here no corrections to the pure case are obtained. The method employed uses a field-theoretic calculation (in terms of Goldstone diagrams) of the ground-state energy of an effective many-body Hamiltonian. The validity of the replica method is tested numerically.

KEY WORDS: Wetting; two-dimensional systems; random systems; interfaces.

1. INTRODUCTION

The study of different aspects of wetting phenomena has generated considerable research activity lately (see Refs. 1 for recent reviews). One of these aspects is the wetting transition. This transition occurs when one of the phases of a two- (or many-) component system at coexistence, enclosed in a container, forms a macroscopically thick film on the wall (substrate) of the container. This film can be formed continuously, in which case the transition is second order. A discontinuous jump of the thickness signals a first-order transition.

¹ Department of Physics, Clarkson University, Potsdam, New York 13676.

² Service de Physique Théorique, CEN-Saclay, 91191 Gif-sur-Yvette, France.

³ Institut für Theoretische Physik A, RWTH Aachen, 5100 Aachen, Federal Republic of Germany.

⁴ Department of Nuclear Physics and Department of Electronics, Weizmann Institute of Science, 76100 Rehovot, Israel.

If the transition is discontinuous, a first-order transition line extends into the region where the system is not at coexistence. This line is called the prewetting line. It terminates at a critical point, which belongs to the Ising universality class.⁽²⁾ The effect of substrate randomness on this transition has been studied within the mean field theory.⁽²⁾ The surprising result of this study is that the prewetting critical point of the pure system is shifted and eventually, if randomness is strong enough, disappears. When it disappears, the first-order wetting transition becomes second order. This prediction still awaits experimental verification.

If the wetting transition in the pure system is second order, its nature may be changed by bulk randomness, as has been shown recently by exact calculations⁽³⁾ and general scaling arguments.⁽⁴⁾ On the contrary, in the case of substrate randomness, the transition of the pure system is not affected, as has been demonstrated by using the Harris criterion⁽⁵⁾ and mean field calculations.⁽²⁾ The results of Ref. 2 apply to systems with bulk dimensionality larger than two. The two-dimensional case is marginal, since in the pure system the specific heat exponent α is zero,^(6,7) and the Harris criterion is not very useful. However, $\alpha = 0$ corresponds to a finite jump in the specific heat (and not to a logarithmic singularity, as in the two-dimensional Ising model); therefore, one expects that the effect of randomness is rather weak.

In the present work, we study in detail the effect of substrate randomness in two bulk dimensions (2d). We consider a restricted solid-on-solid (RSOS) model. This model describes correctly the universal features of the second-order wetting transition in the pure 2d system. To treat quenched randomness, we use the replica trick, which results in an effective many-body Hamiltonian. To determine the free energy of the random system, we calculate the ground-state energy of the many-body Hamiltonian. This is done by using the Goldstone time-ordered perturbation theory.⁽⁸⁻¹⁰⁾ The perturbative expansion is performed in terms of the cumulants of the distribution function characterizing the randomness. The perturbation series for the singular part of the free energy can be summed up. In this way we obtain an exact expression for the quenched free energy in the critical region. As a result, we prove that substrate randomness is indeed irrelevant, in the sense that it leads “only” to logarithmic corrections in the free energy and specific heat. The perturbative analysis can be carried out also for the width of the wetting layer. Here, according to our calculations, the results for the pure case are not changed at all. As regards the value of the critical wetting temperature, we prove that it is that of the annealed system. Our results are exact, and valid for arbitrary randomness.

The paper is organized as follows. In Section 2, we define our model, and give its solution in the pure case. Section 3 contains the derivation of

the quenched free energy in an easy way, without the machinery of field theory. It leads to the correct result, but the justification of some steps of the calculation can be given only in later sections. In Section 4, we derive the many-body Hamiltonian, whose ground-state energy we calculate, using the Goldstone perturbation theory, which is reviewed in Section 5. Section 6 contains the exact calculation of the quenched free energy using Goldstone diagrams, whereas in Section 7 we calculate the width of the wetting layer. In Section 8 we present numerical results, with which we intend to prove the validity of the replica trick. Finally, in Section 9 we discuss the relation of our model to some other random models, and make a few concluding remarks.

A short version of the present work (restricted to the case of Gaussian disorder) has been recently published.⁽¹¹⁾

2. THE MODEL AND THE NONRANDOM (ANNEALED) CASE

In this section, we define the model we use to study the quenched random wetting problem. Since in the next sections this model is solved perturbatively in the strength of randomness, we give here the solution of the pure case. This formally corresponds to the annealed case, as will be demonstrated.

We consider a restricted solid-one-solid (RSOS) model, with an arbitrary distribution of wall potentials. The partition function of the system reads

$$\mathcal{Z} = \sum_{\{h_i=0,1,\dots,L\}} \exp\left(-\beta J \sum_{i=1}^N |h_{i+1} - h_i| + \beta \sum_{i=1}^N u_i \delta_{h_i,0}\right) \quad (1)$$

Here L is the vertical size of the container and N is its horizontal size, the wall being horizontal. u_i is the random substrate potential at site i along the wall. We assume that u_i are a set of independent random variables, all with the same distribution $\rho(u) du$. The term $|h_{i+1} - h_i|$ takes only values 0 and 1.

The quenched free energy is obtained by averaging $\ln \mathcal{Z}$ over the distribution of u_i ; in order to evaluate it, we introduce replicas:

$$\overline{\ln \mathcal{Z}} = \left. \frac{d}{dn} \overline{\mathcal{Z}^n} \right|_{n=0} \quad (2)$$

In Eq. (2), the bar stands for the average over disorder. Performing this average, we obtain

$$\overline{\mathcal{Z}^n} = \sum_{\{h_i^z\}} \exp\left[-\beta J \sum_{i=1}^N \sum_{z=1}^n |h_{i+1}^z - h_i^z| + \beta \sum_{i=1}^N \mathcal{U}\left(\sum_{z=1}^n \delta_{h_i^z,0}\right)\right] \quad (3)$$

Here we define the function \mathcal{U} by

$$\exp[\beta\mathcal{U}(x)] = \int du \rho(u) e^{\beta ux} \quad (4)$$

It will be useful to use the series expansion of $\mathcal{U}(x)$ as

$$\mathcal{U}(x) = \sum_{k=0}^{\infty} C_k \frac{x^k}{k!} \quad (5)$$

where the C_k are the cumulants of the distribution ρ ,

$$\begin{aligned} C_0 &= 0 \\ C_1 &= \bar{u} \\ C_2 &= \beta(\overline{u^2} - \bar{u}^2) = \beta V \end{aligned} \quad (6)$$

In the thermodynamic limit ($N \rightarrow \infty$), the problem of calculating $\overline{\mathcal{Z}^n}$ reduces to finding the largest eigenvalue A_n of the transfer matrix

$$\begin{aligned} M_n(\{h_\alpha\}, \{h'_\alpha\}) &= \exp\left[-\beta J \sum_{\alpha=1}^n |h_\alpha - h'_\alpha| + \beta\mathcal{U}\left(\sum_{\alpha=1}^n \delta_{h'_\alpha, 0}\right)\right] \\ &= T_n(\{h_\alpha\}, \{h'_\alpha\}) \exp[W(\{h_\alpha\}, \{h'_\alpha\})] \end{aligned} \quad (7)$$

where

$$T_n(\{h_\alpha\}, \{h'_\alpha\}) = \exp\left(-\beta J \sum_{\alpha=1}^n |h_\alpha - h'_\alpha| + \beta\mathcal{U}_1 \sum_{\alpha=1}^n \delta_{h'_\alpha, 0}\right) \quad (8)$$

and

$$\mathcal{U}_1 = \frac{1}{\beta} (e^{\beta\bar{u}}) = \mathcal{U}(x=1) \quad (9)$$

W in (7) is given by

$$W(\{h_\alpha\}, \{h'_\alpha\}) = \beta \prod_{\alpha=1}^n \delta_{h_\alpha, h'_\alpha} \left[\mathcal{U}\left(\sum_{\alpha=1}^n \delta_{h_\alpha, 0}\right) - \mathcal{U}_1 \sum_{\alpha=1}^n \delta_{h_\alpha, 0} \right] \quad (10)$$

If the distribution $\rho(u)$ is chosen to be Gaussian, with mean \bar{u} and variance V , the expression in the square brackets of (10) reduces to

$$\beta V \sum_{1 \leq \alpha < \beta \leq n} \delta_{h_\alpha, 0} \delta_{h_\beta, 0} \quad (11)$$

At the same time, (9) takes the form

$$\mathcal{U}_1 = \bar{u} + \frac{1}{2} \beta V \quad (12)$$

Quenched averaging then introduces an effective interaction between replicas, as is shown by (11). In the case of a general distribution there will be “ k -body” interactions with $k = 2, 3, \dots, n$.

Then

$$\overline{\mathcal{Z}^n} = \text{Tr } M_n^N \underset{N \rightarrow \infty}{\sim} A_n^N \quad (13)$$

We denote in operator form

$$\exp W(\{h_\alpha\}, \{h'_\alpha\}) = (e^{-V})(\{h_\alpha\}, \{h'_\alpha\}) \quad (14)$$

so that

$$M_n = T_n e^{-V} \quad (15)$$

We define E_0 by

$$A_n = (1 + 2e^{-\beta J})^n e^{-E_0(n)} \quad (16)$$

The critical wetting point is obtained when $A_n = (1 + 2e^{-\beta J})^n$, which demarcates the localized and delocalized phases. In the critical region, $E_0 \rightarrow 0$, and E_0 can be related to the relevant length scales of the problem.

We will evaluate E_0 by performing a perturbative expansion in powers of the cumulants C_k , and it is therefore necessary to study the spectrum of T_n . Here T_n is the transfer matrix of the annealed case, which in turn is equivalent to the pure ($n = 1$) case, since T_n is the n th tensorial power of the operator T_1 .

The spectrum of T_1 is simply obtained by solving for the eigenvalue equation, which takes the form

$$\sum_{h'=0}^L [\delta_{hh'} + t(\delta_{h',h+1} + \delta_{h',h-1})][1 + \delta_{h',0}(y-1)] \phi_\lambda(h') = \varepsilon_\lambda \phi_\lambda(h) \quad (17)$$

Here $t = e^{-\beta J}$, $y = e^{\beta \mathcal{U}_1}$. We will also use the notation

$$\begin{aligned} \varepsilon_h &= 1/\sqrt{y} & \text{if } h = 0 \\ &= 1 & \text{if } h \neq 0 \end{aligned}$$

The spectrum of T_1 (in the dry phase, i.e., when $\langle h \rangle < \infty$) consists of one localized state $\phi_0(h)$ and a set of L delocalized states $\phi_q(h)$.

More precisely, it is easy to see from (17) that

$$\phi_0(h) = \varepsilon_h \left(\frac{1}{y} + \frac{1}{e^{2\mu} - 1} \right)^{-1/2} e^{-\mu h} \quad (18)$$

with eigenvalue

$$e_0 = 1 + 2t \cosh \mu = y(1 + te^{-\mu}) \quad (19)$$

Then (19) defines μ as a function of t and y .

The critical wetting occurs for $\mu = 0$, and thus the criticality condition reads

$$y^* = \frac{1 + 2t^*}{1 + t^*} \quad (20)$$

Close to the critical point, $\mu \rightarrow 0$, and one obtains

$$\begin{aligned} \mu &\simeq [y(1+t) - (1+2t)]/yt \\ e_0 &\simeq (1+2t)(1+\gamma\mu^2) \end{aligned} \quad (21)$$

where $\gamma = t/(1+2t)$. For future use, note that

$$f_0^2 = \phi_0^2(0) \simeq 2\mu/y \quad (\mu \rightarrow 0) \quad (22)$$

For the extended states $\phi_q(h)$, one gets

$$\phi_q(h) = \varepsilon_h (2/L)^{1/2} \sin[q(h-L)] \quad (23)$$

with eigenvalues

$$e_q = 1 + 2t \cos q \quad (24)$$

The matching condition at $h=0$

$$y \sin(-qL) + yt \sin q(1-L) = (1 + 2t \cos q) \sin(-qL) \quad (25)$$

implies a ‘‘quantization’’ condition on the admissible values of q :

$$\tan qL = \frac{yt \sin q}{y(1+t \cos q) - (1+2t \cos q)} \quad (26)$$

This is an equation of degree $2L+2$ in e^{iq} , which has $(L+1)$ solutions with $0 \leq q \leq \pi$.

The critical domain is characterized by long-range correlations, and thus only the small- q eigenstates are important. For small q , we have

$$\tan qL \simeq \frac{ytq}{y(1+t) - (1+2t) - q^2(yt/2 - t)} \quad (27)$$

so that

$$\sin^2 qL \simeq \frac{q^2}{q^2 + \mu^2}, \quad e_q \simeq (1 + 2t)(1 - \gamma q^2) \quad (28)$$

For future reference

$$f_q^2 = \phi_q^2(0) \simeq \frac{2}{yL} \frac{q^2}{q^2 + \mu^2} \quad (29)$$

Equation (29) is valid in the critical region, i.e., for q and $\mu \rightarrow 0$. In the thermodynamic limit, we will replace sums by integrals, according to

$$\frac{1}{L} \sum_q \rightarrow \frac{1}{\pi} \int_0^\pi dq$$

With the above results, all observables can be evaluated. In the critical region, on the dry side of the transition, we obtain

$$\langle h \rangle \simeq \frac{1}{\mu}, \quad \xi_{||} \sim \frac{1}{e_0 - e_\mu} \sim \frac{1}{\mu^2} \quad (30)$$

The free energy is given by

$$-\beta f = \lim_{N \rightarrow \infty} (-\beta F/N) = \ln(1 + 2t) + \gamma \mu^2 \quad (31)$$

On the wet side of the transition, the width $\langle h \rangle$ of the wetting layer remains infinite, and

$$-\beta f = \lim_{N \rightarrow \infty} (-\beta F/N) = \ln(1 + 2t) \quad (32)$$

Relations (31) and (32) imply a jump in the specific heat.^(6,7)

In the critical region, it is easily seen that one can write

$$T_1 = (1 + 2t)e^{-H_0} \quad (33)$$

where the operator H_0 is given by

$$H_0 = -\gamma \mu^2 |\phi_0\rangle \langle \phi_0| + \sum_{q>0} \gamma q^2 |\phi_q\rangle \langle \phi_q| \quad (34)$$

3. CRITICAL BEHAVIOR OF THE QUENCHED RANDOM SYSTEM. THE EASY WAY

In this section we present a simple perturbative derivation of the critical behavior of the quenched random system. It is only meant for

pedagogical purposes, and the justification of essential steps will be given later. In this section, we restrict the discussion to Gaussian randomness.

To investigate the critical behavior of the quenched random system, we need the largest eigenvalue A_n of the transfer matrix M_n , given by (7) and (15).

We perform a perturbative expansion of A_n in powers of V around the ground state of the annealed system. We write

$$M_n = T_n - T_n V + \dots \quad (35)$$

A standard perturbation theory gives

$$A_n = e_0^n \langle 0 | 1 - V + VGV - VGVGV + \dots | 0 \rangle \quad (36)$$

where

$$G = \frac{1}{e_0^n T_n^{-1} - 1} (1 - |0\rangle\langle 0|) \quad (37)$$

contains a projector, indicating that all the intermediate n -particle states are excited states. Here $|0\rangle$ denotes the noninteracting ground state of then n -particle system, which is a direct product of the $|\phi_0\rangle$ states used in (34). The first nontrivial term in (36) is

$$\langle 0 | VGV | 0 \rangle = \frac{1}{2} n(n-1) (\beta^2 V)^2 f_0^4 I \quad (38)$$

where

$$I = \sum_{q_1 q_2} \frac{f_{q_1}^2 f_{q_2}^2}{e_0^2 (e_{q_1} e_{q_2})^{-1}} \quad (39)$$

For small μ and q , using the results of the preceding section, one obtains

$$\begin{aligned} I &\simeq \frac{4(1+2t)}{y^2 t} \int_0^\pi \frac{dq_1}{\pi} \int_0^\pi \frac{dq_2}{\pi} \frac{q_1^2}{\mu^2 + q_1^2} \frac{q_2^2}{\mu^2 + q_2^2} \frac{1}{2\mu^2 + q_1^2 + q_2^2} \\ &\simeq \frac{2(1+2t)}{ty^2 \pi} \ln \frac{1}{\mu} \end{aligned} \quad (40)$$

It can be shown (see below) that, at any order in the perturbation expansion, the most divergent terms are those where, in the intermediate states, only two particles (replicas) are excited. Due to the factorized nature of the interaction V [see Eqs. (11) and (14)], the integrals separate, and to leading order one obtains

$$\begin{aligned}
A_n &= e_0^n \left\{ 1 + \frac{1}{2} \beta^2 V n(n-1) f_0^4 [1 + \beta^2 VI + (\beta^2 VI)^2 + \dots] \right\} \\
&= e_0^n \left\{ 1 + \frac{1}{2} \frac{\beta^2 V n(n-1) f_0^4}{1 - \beta^2 VI} \right\}
\end{aligned} \tag{41}$$

Using (2), (13), (40), and (41), for the quenched free energy in the small- μ limit, we get

$$-\beta f = \ln(1 + 2t) + \mu^2 \gamma \left[1 + O(V^3) + \frac{2\pi}{|\ln(T_w - T)|} + O\left(\frac{1}{\ln^2(T_w - T)}\right) \right] \tag{42}$$

Here T_w is the critical wetting temperature and $\mu \sim (T_w - T)$. Comparing with (31) for the annealed case, it follows that the jump in the specific heat has a $1/\log$ correction. Note that the critical temperature of the quenched system is the same as that of the annealed system. (The reason for this will be discussed later in more detail.)

It is the purpose of the next sections to prove more rigorously that the result (42) gives the correct critical behavior for arbitrary disorder.

4. SECOND-QUANTIZED REPRESENTATION FOR THE QUENCHED DISORDERED SYSTEM

In what follows, we construct a second-quantized representation for M_n , which will prove to be very convenient for performing the calculation of A_n in terms of Goldstone diagrams.

Since we expect (from the Harris criterion) that disorder is marginally irrelevant in our system, it is reasonable to assume that both $\langle H_0 \rangle$ and $\langle V \rangle$ will go to zero with E_0 . (This assumption will indeed be checked at the end of our calculations.) With this proviso, it is easy to see, using the Baker–Campbell–Hausdorff formula, that

$$M_n = (1 + 2t)^n e^{-H_{0n}} e^{-V} = (1 + 2t)^n e^{-(H_{0n} - W)} \tag{43}$$

with $W = -V + O(E_0^2)$. Thus, in the critical region ($E_0 \rightarrow 0$), diagonalizing M_n just amounts to diagonalizing the operator $H = H_{0n} - W$. All operators now act in the space of n particles. Since T_n is a tensor product of T_1 operators, H_{0n} is readily seen to be a sum of one-body operators H_0 , given by (34), whereas from (10), W is a many-body operator. For arbitrary disorder

$$W = \beta^2 \sum_{1 \leq \alpha < \beta \leq n} C_2 \delta_{h_{\alpha,0}} \delta_{h_{\beta,0}} + 3\text{-body} + \dots \tag{44}$$

We now proceed to represent H in a second-quantized form. The n particles are to be considered as distinguishable, since they are not constrained to any symmetrization condition *a priori*. However, since the Hamiltonian H is totally symmetric, so is its ground state. We thus introduce bosonic creation and annihilation operators ψ_λ^\dagger and ψ_λ , where λ denotes the label of the single-particle eigenstates of H_0 .

In the bosonic Fock space, Eq. (34) becomes

$$H_0 = -\gamma\mu^2\psi_0^\dagger\psi_0 + \sum_{q>0} \gamma q^2 \psi_q^\dagger \psi_q \quad (45)$$

and similarly, the interaction W can be written as

$$\begin{aligned} W = & \frac{1}{2} \sum_{\lambda\eta\nu\rho} \langle \lambda\eta | W_2 | \nu\rho \rangle \psi_\lambda^\dagger \psi_\eta^\dagger \psi_\nu \psi_\rho \\ & + \frac{1}{3!} \sum_{\substack{\lambda_1\lambda_2\lambda_3 \\ \nu_1\nu_2\nu_3}} \langle \lambda_1\lambda_2\lambda_3 | W_3 | \nu_1\nu_2\nu_3 \rangle \psi_{\lambda_1}^\dagger \psi_{\lambda_2}^\dagger \psi_{\lambda_3}^\dagger \psi_{\nu_1} \psi_{\nu_2} \psi_{\nu_3} \\ & + 4\text{-body} + \dots + \text{many-body} + \dots \end{aligned} \quad (46)$$

with, for instance,

$$\begin{aligned} \langle \lambda\nu | W_2 | \nu\rho \rangle &= \beta^2 C_2 \sum_{h_1 h_2 h_3 h_4} \delta_{h_1, h_3} \delta_{h_2, h_4} \delta_{h_1, 0} \delta_{h_2, 0} \\ &\quad \times \phi_\lambda(h_1) \phi_\eta(h_2) \phi_\nu(h_3) \phi_\rho(h_4) \\ &= \beta^2 C_2 f_\lambda f_\eta f_\nu f_\rho \end{aligned} \quad (47)$$

$$\langle \lambda_1\lambda_2\lambda_3 | W_3 | \nu_1\nu_2\nu_3 \rangle = \beta^3 C_3 f_{\lambda_1} f_{\lambda_2} f_{\lambda_3} f_{\nu_1} f_{\nu_2} f_{\nu_3} \quad (48)$$

In order to calculate the ground-state energy of H , we perform a perturbation expansion in powers of W . It is well known that perturbation expansion for a system with a *fixed number of bosons* is cumbersome to perform. This is due to the fact that there is no Wick theory for canonical systems of bosons, even at zero temperature. Such a Wick theorem, however, exists for the ground state of a fixed number of fermions, and we shall thus transform our bosonic problem into an equivalent fermionic problem, using the so called “high spin trick.”⁽¹²⁾

Since the unperturbed bosonic ground state is a condensate with all the n bosons in the state $|\phi_0\rangle$, the idea is to replace the n bosons by a set of n fermions, which carry the same quantum numbers as the bosons, plus an additional color degree of freedom (i.e., high spin), denoted by σ . This

color index ranges from 1 to n . Let us then consider the fermionic Hamiltonian

$$\begin{aligned}
H_F = & \sum_{\sigma=1}^n \left[-\gamma \mu^2 \psi_{0\sigma}^+ \psi_{0\delta} + \sum_q \gamma q^2 \psi_{q\sigma}^+ \psi_{q\sigma} \right] \\
& + \frac{1}{2} \sum_{\substack{\lambda\eta\nu\rho \\ \sigma_1\sigma_2}} \langle \lambda\eta | W_2 | \nu\rho \rangle \psi_{\lambda\sigma_1}^+ \psi_{\eta\sigma_2}^+ \psi_{\rho\sigma_2} \psi_{\nu\sigma_1} \\
& + \frac{1}{3!} \sum_{\sigma_1\sigma_2\sigma_3} \sum_{\lambda_1\lambda_2\lambda_3} \sum_{\mu_1\mu_2\mu_3} \langle \lambda_1\lambda_2\lambda_3 | W_3 | \mu_1\mu_2\mu_3 \rangle \\
& \times \psi_{\lambda_1\sigma_1}^+ \psi_{\lambda_2\sigma_2}^+ \psi_{\lambda_3\sigma_3}^+ \psi_{\mu_3\sigma_3} \psi_{\mu_2\sigma_2} \psi_{\mu_1\sigma_1} \\
& + \text{many-body}
\end{aligned} \tag{49}$$

Here $\psi_{\lambda\sigma}^+$ and $\psi_{\lambda\sigma}$ are creation and annihilation operators for a fermion in state $|\phi_\lambda\rangle$ with color σ .

The unperturbed ground state of H_F (with eigenvalue $n\varepsilon_0$) is given by

$$|\Phi_0\rangle = \prod_{\sigma=1}^n \psi_{0\sigma}^+ |0\rangle \tag{50}$$

which factorizes into a spatially symmetric wave function (all particles in states $|\phi_0\rangle$) and an antisymmetric wave function in the color index. The Hamiltonian H_F is diagonal in color space by construction. It cannot therefore change the color wave function of any state.

The true ground state $|\varphi_0\rangle$ of H_F can be obtained by using

$$r^{-TH_F} |\Phi_0\rangle \underset{T \rightarrow \infty}{\simeq} e^{-Tn\varepsilon_0} \langle \varphi_0 | \Phi_0 \rangle |\varphi_0\rangle \tag{51}$$

Since e^{-TH_F} does not change the color wave function of $|\Phi_0\rangle$, $e^{-TH_F} |\Phi_0\rangle$ is also spatially symmetric and color antisymmetric. We obtain in this way that the spatial part of $e^{-TH_F} |\Phi_0\rangle$ is identical to the bosonic ground-state wave function.

We are thus led to calculate the ground-state energy of H_F by performing a perturbation expansion in powers of W from the unperturbed ground state $|\Phi_0\rangle$.

This perturbation expansion can be done by means of Feynman or Goldstone diagrams. It turns out that the latter are more appropriate for the present problem; therefore, in the next section we review the Goldstone expansion and diagrams.

5. GOLDSTONE DIAGRAMS

We review the Goldstone perturbation expansion^(8, 10) for the ground-state energy of a system of n fermions. The Hamiltonian is

$$H_F = H_{0n} + H_1 \quad (52)$$

H_{0n} is a sum of operators given by (45), where now the operators carry an extra index σ [see (49)]. H_1 can be identified from (49). The explicit expression for the matrix elements in (49) is given by (47) and (48). The unperturbed ground state is given by (50):

$$H_{0n}|\Phi_0\rangle = n\varepsilon_0|\Phi_0\rangle \quad (53)$$

[For small μ , $\varepsilon_0 = -\gamma\mu^2$, as can be seen from (33) and (34).]

For the exact ground state of H_F , we write

$$H_F|\varphi_0\rangle = E_0|\varphi_0\rangle \quad (54)$$

Standard perturbation theory gives

$$\begin{aligned} E_0 = n\varepsilon_0 + \langle\Phi_0|H_1|\Phi_0\rangle + \langle\Phi_0|H_1\tilde{G}H_1|\Phi_0\rangle + \langle\Phi_0|H_1\tilde{G}H_1\tilde{G}H_1|\Phi_0\rangle \\ - \langle\Phi_0|H_1|\Phi_0\rangle \times \langle\Phi_0|H_1\tilde{G}_2H_1|\Phi_0\rangle + \dots \end{aligned} \quad (55)$$

Here

$$\tilde{G} = P/(n\varepsilon_0 - H_{0n})$$

is then Green's function [compare with (37)] and

$$P = 1 - |\Phi_0\rangle\langle\Phi_0|$$

is a projector outside the Fermi sea. It is simple to give a graphical interpretation to Eq. (55). Each term is read from right to left. A typical term $P H_1$ acting on $|\Phi_0\rangle$ leads to a new Slater determinant. For example,

$$P\psi_{\lambda_1\sigma_1}^+\psi_{\lambda_2\sigma_2}^+\psi_{\mu_2\sigma_2}\psi_{\mu_1\sigma_1}|\Phi_0\rangle$$

Here two particles of $|\Phi_0\rangle$ in states $\mu_1\sigma_1$ and $\mu_2\sigma_2$ have been replaced by two particles in states $\lambda_1\sigma_1$ and $\lambda_2\sigma_2$. Since $|\Phi_0\rangle$ is a Fermi sea, the states $\mu_1\sigma_1$ and $\mu_2\sigma_2$ must be hole states, i.e., belong to the Fermi sea, whereas

the states $\lambda_1\sigma_1$ and $\lambda_2\sigma_2$ must be particle states, i.e., above the Fermi sea. The new state is an eigenstate of H_{0n} with energy

$$E_1 = n\varepsilon_0 - \varepsilon_{\mu_1} - \varepsilon_{\mu_2} + \varepsilon_{\lambda_1} + \varepsilon_{\lambda_2}$$

($\varepsilon_q = +\gamma q^2$ for small q). Thus, multiplying this state by $(n\varepsilon_0 - H_{0n})^{-1}$ merely multiplies it by an energy denominator

$$\frac{1}{\sum_{\text{particles}} \varepsilon_{\text{particles}} - \sum_{\text{holes}} \varepsilon_{\text{holes}}}$$

Applying again PH_1 to this states transforms in into a new Slater determinant, with new particles and holes and appropriate energy. Finally, applying $\langle \Phi_0 | H_1$ to this state must remove all particle-hole excitations from the intermediate state, so as to project it back to $|\Phi_0\rangle$.

It is convenient to represent hole states by downgoing lines and particle states by upgoing lines. Each operator H_1 is represented by a vertex. For example the term proportional to $\langle \lambda\eta | W_2 | \nu\rho \rangle$ in (49) can be represented by the diagram of Fig. 1a. A three-body operator corresponds to the diagram of Fig. 1b. It can be shown⁽⁹⁾ that the perturbation expansion (55) is obtained graphically by drawing any number of vertices (of any type), and connecting them in all possible ways. Between any number of consecutive vertices, there is an energy determinator, equal to the sum of energies of the holes. There are combinatorial factors and signs, which we do not details,⁽⁸⁻¹⁰⁾ and the final expression is to be summed over all quantum numbers present in the graph.

A priori, such graphs can be disconnected. For example, the last term in (55) is obviously a disconnected diagram. However, Goldstone proved⁽⁸⁾ that all disconnected diagrams cancel, and thus the ground-state energy of the system is the sum of all connected diagrams.

We give now more precisely the rules for calculating these Goldstone diagrams.

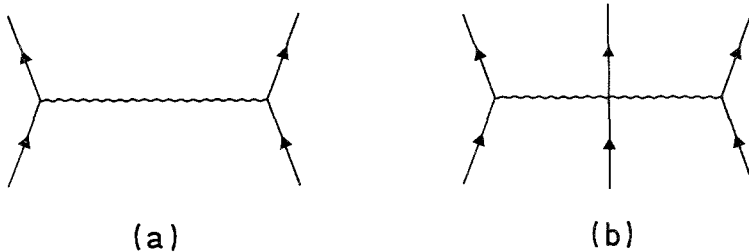


Fig. 1. Graphical representation of (a) a two-particle interaction and (b) a three-particle interaction in (46).

1. An upward-directed line represents a particle state (state above the Fermi sea) (q, σ) . A downgoing line corresponds to a hole state (state in the Fermi sea $(0, \sigma)$).

2. A matrix element $\langle \lambda_1 \lambda_2 \cdots \lambda_p | W_p | \mu_1 \cdots \mu_p \rangle$ is represented by a horizontal wavy line, with p outgoing lines carrying indices $\lambda_1 \lambda_2 \cdots \lambda_p$, and p incoming lines with indices $\mu_1 \mu_2 \cdots \mu_p$.

3. Between two vertices there is an energy denominator, which equals the sum of the particle energies minus the sum of the hole energies.

4. The sign of the diagram is given by $(-1)^{N_h + N_c + V - 1}$, where N_h , N_c , and V stand, respectively, for the numbers of hole lines, fermion loops, and vertices.

5. Summation over the momenta q and color indices σ has to be performed.

Since color is conserved at each vertex, summation over it is trivial, and simply multiplies the contribution of the diagram by n^{N_c} . With those rules the contribution of the graph of Fig. 2 is

$$-(\beta^2 C_2)^2 n^2 f_0^4 L^2 \int_0^\pi \frac{dq_1}{\pi} \int_0^\pi \frac{dq_2}{\pi} \frac{f_{q_1}^2 f_{q_2}^2}{\gamma(2\mu^2 + q_1^2 + q_2^2)} \quad (56)$$

Since we are interested in evaluating $(\partial E_0 / \partial n)|_{n=0}$, we see that we have to retain only those diagrams that are proportional to n , i.e., graphs with only one fermion loop.

Figure 3 shows some of these diagrams.

To conclude this section, let us note that, due to the separable nature of the interactions, each line carries a factor f_λ^2 , provided we associate a factor $\beta^p C_p / p!$ to a p -body vertex.



Fig. 2. Graphical representation of the analytical expression given by (56).

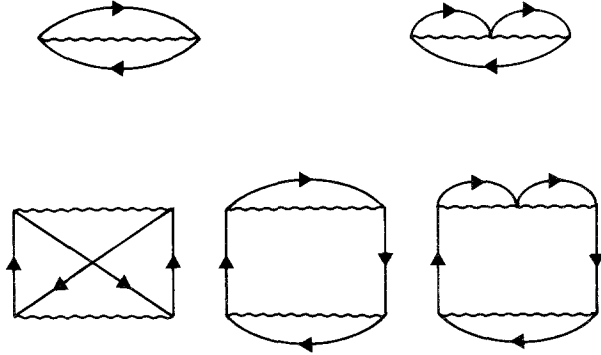


Fig. 3. Some Goldstone diagrams contributing to the ground-state energy.

6. GROUND-STATE ENERGY

Let us consider a generic diagram, with one fermion loop, contributing to the ground-state energy.

Such a diagram has N_p particles lines, N_h hole lines, and V_m vertices of m -body interactions, $m \geq 2$. The contribution of such a diagram to the ground-state energy has the form

$$\delta E_0 = \prod_{m \geq 2} \left(\frac{\beta^m C_m}{m!} \right)^{V_m} (-1)^{N_h + V} L^{N_p} \int_0^A \prod_{i=1}^{N_p} \frac{dq_i}{\pi} (f_0^2)^{N_h} \times \prod_{i=1}^{N_p} f_{q_i}^2 \prod_{j=1}^{V-1} \frac{1}{\sum \epsilon_{\text{particles}} - \sum \epsilon_{\text{holes}}} \tag{57}$$

Here $V = \sum_{m \geq 2} V_m$ is the total number of vertices. A denotes some finite ultraviolet (UV) cutoff. The last product in (57), $\prod_{j=1}^{V-1}$, contains the energy denominators between the j th and $(j+1)$ th vertices. [Remember that (57) contains only one fermion loop.]

Since q may go to 0, we see that when $\mu \rightarrow 0$, (57) may become infrared (IR)-divergent. In fact, these IR divergences signal the onset of the wetting transition, and the critical behavior will be governed by the most IR divergent graphs. As is usual in the study of phase transitions (see, e.g., Ref. 13), it is useful to transform these IR divergences into UV divergences by a simple changes of scale in the momenta, and analyze the UV behavior of the integrals.

We thus make a change of variables in (57),

$$q_i = \mu x_i$$

and, using (22) and (29), we obtain, up to constant factors,

$$\delta E_0 \sim \mu^{N_h + N_p - 2(V-1)} \int_0^{A/\mu} \prod_{i=1}^{N_p} \frac{dx_i}{\pi} \prod_{i=1}^{N_p} \frac{x_i^2}{x_i^2 + 1} \prod_{j=1}^{V-1} \frac{1}{\gamma \sum_k x_k^2 + \gamma \sum_k 1} \quad (58)$$

It is now simple to analyze the divergence of the perturbation expansion. We shall use the cutoff A as a momentum scale. Then, simple dimensional analysis shows that

$$[g_m] = [\beta^m C_m] = 2 - m$$

where the brackets indicate dimension, in units of A (inverse length).

Only those vertices with positive or vanishing dimension are relevant at criticality, i.e., can lead to divergences. We thus reach the important result that only two-body vertices may affect the critical behavior, all higher order interactions being irrelevant. Consequently, the critical behavior of the 2d (substrate) disordered wetting problem is universal: it depends on the distribution of the surface fields only through its first two cumulants.

Thus, we may reduce the Hamiltonian to

$$H = H_{0n} + \frac{g_2}{2} \sum_{\lambda_1 \lambda_2 \mu_1 \mu_2} f_{\lambda_1} f_{\lambda_2} f_{\mu_1} f_{\mu_2} \psi_{\lambda_1 \sigma_1}^+ \psi_{\lambda_2 \sigma_2}^+ \psi_{\mu_2 \sigma_2} \psi_{\mu_1 \sigma_1}$$

The contribution of a graph becomes

$$\delta E_0 \sim (g_2)^V \frac{\mu^2}{y^{N_h + N_p}} I\left(\frac{A}{\mu}\right) \quad (59)$$

Here we used the topological relation

$$4V = 2N_h + 2N_p$$

V now denotes the total number of two-body vertices. $I(A/\mu)$ is the integral in (58).

The marginality of the coupling g_2 guarantees that $I(A/\mu)$ is at most logarithmically divergent, and indeed the degree of divergence of $I(A/\mu)$ is given by

$$\delta(I) = N_p - 2(V-1) = 2 - N_h \quad (60)$$

Thus, all diagrams with three or more hole lines are UV-convergent, and cannot affect the critical behavior, whereas diagrams with two hole lines may.

We thus conclude that the singular part of the free energy is the sum of all diagrams with two hole lines, i.e., the sum of all ladder diagrams shown in Fig. 4. (A line connecting two ends of the same vertex is a hole line.)

Because of the factorized nature of the two-body interaction, each ladder diagram can be factorized, and the sum in Fig. 4 is a geometric series. This finally leads to

$$\frac{\partial E_0}{\partial n} \Big|_{n=0} = \gamma\mu^2 - g_2\mu^2 \left(\frac{2}{y}\right)^2 \frac{1}{1 - g_2 I} \tag{61}$$

Here I is the basic “building block” of the series, given by (40). Consequently, the free energy, close to the critical point ($\mu = 0$), is given by

$$-\beta f = \ln(1 + 2t) + \frac{\mu^2 t}{1 + 2t} \left(S_2 + \frac{2\pi}{\ln(1/\mu)} \right) + O(\mu^3) \tag{62}$$

S_2 in the above expression is the sum of all convergent graphs with two-body interactions. The $O(\mu^3)$ is the contribution of the three-body, etc., vertices, and is indeed irrelevant for small μ , as can be seen from (58). [A three-body vertex contains at least three hole lines, in which case the corresponding integral in (58) is UV-convergent according to (60).] The result (62) for the free energy implies that the behavior in the specific heat at the transition is

$$\Delta C = \Delta C_0 \left(S_2 + \frac{2\pi}{\ln(1/\mu)} \right)$$

where ΔC_0 is the jump in the absence of disorder. It is interesting to point out that, whereas S_2 contains g_2 (which in turn depends on \mathcal{U}_2), the singular part of the free energy and of the specific heat is completely independent of the strength of disorder.

One remark concerning the above results is necessary. It has been assumed that the critical point of the quenched disordered system is the

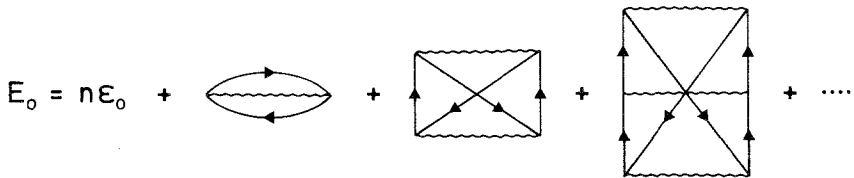


Fig. 4. The infinite series of ladder diagrams for the ground-state energy close to the transition.

same as that of the annealed system, namely criticality is given by $\mu = 0$. This is correct if the squared “mass” μ^2 in the bare Hamiltonian (45) is not renormalized by the interactions. More precisely, for the above results to hold, one needs $\mu_R(\mu = 0) = 0$, where μ_R is the renormalized mass. It will be proved in the next section that indeed $\mu_R(\mu = 0) = 0$.

7. WIDTH OF THE WETTING LAYER

The width w of the wetting layer is obtained by calculating the average of the height variable h_α for any α (and then letting $n \rightarrow 0$). Choosing $\alpha = 1$, in the second-quantized formalism, we obtain

$$w = \frac{\langle \varphi_0 | \hat{h}_1 | \varphi_0 \rangle}{\langle \varphi_0 | \varphi_0 \rangle} = \sum_{\lambda\mu} \langle \lambda, \sigma = 1 | \hat{h} | \mu, \sigma = 1 \rangle \frac{\langle \varphi_0 | \psi_\lambda^+ \psi_\mu | \varphi_0 \rangle}{\langle \varphi_0 | \varphi_0 \rangle} \quad (63)$$

We are then led to calculate the average of a one-particle operator $\psi_\lambda^+ \psi_\mu$. The perturbation theory for such an average can be worked out quite similarly to that presented for the ground-state energy. Standard perturbation theory for a one-particle operator K leads to

$$\begin{aligned} \langle K \rangle &= \langle \Phi_0 | K | \Phi_0 \rangle - \langle \Phi_0 | K | \Phi_0 \rangle \langle \Phi_0 | H_1 \tilde{G}^2 H_1 | \Phi_0 \rangle \\ &\quad + \langle \Phi_0 | K \tilde{G} H_1 | \Phi_0 \rangle + \langle \Phi_0 | H_1 \tilde{G} K | \Phi_0 \rangle \\ &\quad + \langle \Phi_0 | K \tilde{G} H_1 \tilde{G} H_1 | \Phi_0 \rangle + \langle \Phi_0 | H_1 \tilde{G} H_1 \tilde{G} K | \Phi_0 \rangle \\ &\quad + \langle \Phi_0 | H_1 \tilde{G} K \tilde{G} H_1 | \Phi_0 \rangle \\ &\quad - \langle \Phi_0 | H_1 | \Phi_0 \rangle [\langle \Phi_0 | K \tilde{G}^2 H_1 | \Phi_0 \rangle + \langle \Psi_0 | H_1 \tilde{G}^2 K | \Phi_0 \rangle] \end{aligned} \quad (64)$$

[Note that the above reduces to (55) if $K = H_0 + H_1$.]

The series (64) can again be represented graphically. Some typical graphs are shown in Fig. 5. Here K is represented by the dotted line with a cross at the end. It can be proved⁽¹⁰⁾ that only connected diagrams give a contribution to (64). It is clear that all diagrams in (64) can be generated from those for the ground-state energy by putting an insertion of K on any of the particle or hole lines. In view of the results of the preceding section, it is now easy to prove that none of these decorated diagrams gives a singular contribution, in the $\mu \rightarrow 0$ limit. Since only diagrams with two hole lines gave a singularity in E_0 , it is sufficient to decorate those diagrams. Consider the first diagram of Fig. 5. Here a particle line has been decorated. Using the rules to evaluate the Goldstone diagrams given in Section 5, the contribution of this diagram is found to be proportional to

$$f_0^4 \int_0^A dq_1 \int_0^A dq_2 \int_0^A dq_3 \frac{f_{q_1}^2 f_{q_2}^2 f_{q_3}^2}{(\mu^2 + q_1^2 + q_2^2)(\mu^2 + q_1^2 + q_3^2)}$$

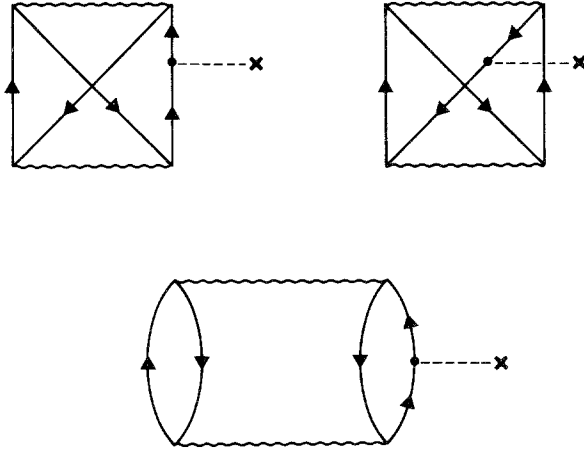


Fig. 5. Some diagrams contributing to the average width of the wetting layer.

For small μ the above expression is proportional to μ ; it vanishes in the $\mu \rightarrow 0$ limit. Now consider the second diagram in Fig. 5. Here a hole line has been decorated. The expression of this diagram is proportional to

$$f_0^6 \int_0^A dq_1 \int_0^A dq_2 \frac{f_{q_1}^2 f_{q_2}^2}{(\mu^2 + q_1^2 + q_2^2)^2}$$

For small μ , the above expression is again proportional to μ . In this way we obtain that, if $\langle \Phi_0 | K | \Phi_0 \rangle$ is singular, the interactions (disorder) do not change this singularity. Applying the above results to (63), we have to evaluate $\langle \Phi_0 | \psi_\lambda^+ \psi_\mu | \Phi_0 \rangle$. This is nonzero only if $\lambda = \mu$, and the state belongs to the Fermi sea.

This means that the singularity of w is given by the singularity of the matrix element of \hat{h} in the ground state of the one-particle system, and so it is exactly the same as in the noninteracting case. We can now easily calculate the renormalized mass μ_R . For this, we need the expectation value of $\psi_{0\sigma}^+ \psi_{0\sigma}$. This is just a special case of a one-particle operator and therefore we immediately obtain

$$\mu_R = \mu + O(\mu^2)$$

which proves that the critical points of the quenched and annealed systems are indeed the same.

8. NUMERICAL RESULTS

The results for the quenched disordered wetting problem obtained in the previous sections could be invalid if the use of the replica trick were not allowed. To test the validity of our results, we present here some numerical results obtained for the RSOS model defined by (1).

We focus our attention on the critical behavior of the free energy per site f and the mean interface height w , and use the natural transfer-matrix formalism introduced in Section 2. This method has proven to be more powerful and efficient than the exact enumeration scheme discussed in our previous publication,⁽¹⁾ which was merely used to determine the critical temperature of the model.

Starting with an arbitrary initial state vector Ω_0 given, e.g., by $(\Omega_0)_h = \delta_{h,0}$, we obtain a sequence of vectors Ω_N by acting on Ω_0 with the ordered product of N transfer operators T_n :

$$\Omega_N = \left(\prod_{n=1}^N T_n \right) \Omega_0 \quad (65)$$

where

$$\begin{aligned} (T_n)_{h,h'} &= \delta_{h,h'} + t(\delta_{h,h'+1} + \delta_{h,h'-1}) & (h \geq 1) \\ &= y_n(\delta_{0,h'} + t\delta_{1,h'}) & (h = 0) \end{aligned} \quad (66)$$

with $t = \exp(-\beta)$ and $y_n = \exp(\beta u_n)$, the substrate potentials u_n having the common distribution $\rho(u) du$.

The critical temperature β_c^{-1} of the model has been shown to be that of an effective annealed model. It is the solution of

$$\int \exp(\beta_c u) \rho(u) du = \frac{1 + 2t_c}{1 + t_c} \quad (67)$$

with $t_c = \exp(-\beta_c)$ (we choose in this section $J = 1$).

We will present numerical results for two classes of substrate potential distributions, namely the *uniform* one:

$$\rho(u) = 1/u_1 \quad (0 < u < u_1) \quad (68a)$$

and the *exponential* (Poissonian) one:

$$\rho(u) = (1/u_2) \exp(-u/u_2) \quad (68b)$$

Equation (67) allows us then to relate the parameters u_1 , u_2 to β_c as follows:

$$\frac{\exp(\beta_c u_1) - 1}{\beta_c u_1} = \frac{1 + 2t_c}{1 + t_c} \quad (69a)$$

$$\beta_c u_2 = \frac{t_c}{1 + 2t_c} \quad (69b)$$

The free energy $f(\beta)$ of the model is simply given by the leading Liapunov exponent of the random sequence Ω_N

$$-\beta f(\beta) = \lim_{N \rightarrow \infty} (N^{-1} \ln \|\Omega_N\|_1) \quad (70a)$$

with

$$\|\Omega_n\|_1 = \sum_{h=0}^{\infty} (\Omega_n)_h \quad (70b)$$

Let us now discuss the critical behavior of this quantity. When the interface is delocalized ($\beta < \beta_c$), we have $f(\beta) \equiv f_e(\beta) = -\beta^{-1} \ln(1 + 2t)$, independently of the potential distribution. For $\beta > \beta_c$ (pinned interface), we define the free energy amplitude

$$R(\beta - \beta_c) = -\beta(f - f_e)/(\beta - \beta_c)^2 \quad (71)$$

This ratio goes to $R(0) = \Delta C / (2\beta_c^2)$ as $\beta \rightarrow \beta_c$, where ΔC is the specific heat jump, which is finite, both in the pure and the random system. It has been shown in Sections 2 and 6 that the way R approaches $R(0)$ is different in the two models:

$$\text{pure case: } R = R(0) + O(\beta - \beta_c) \quad (72a)$$

$$\text{random case: } R = R(0) \left(1 + \frac{2\pi S_2^{-1}}{|\ln(\beta - \beta_c)|} + \dots \right) \quad (72b)$$

where S_2 is a model-dependent constant, which goes to unity in the weak-disorder limit. It also turns out that the logarithmic correction of Eq. (72b) is only observable in a *very* small critical region, which can be estimated from the results of Section 6:

$$\beta - \beta_c < \Delta = \exp[-2\pi/(\lambda v_c)] \quad (73a)$$

where

$$\lambda = 4(1 + t_c)^2 / [t_c(1 + 2t_c)] \quad (73b)$$

and

$$v_c = \beta_c (\partial^2 \mathcal{U}_1 / \partial \beta^2)_{\beta = \beta_c} \quad (73c)$$

For exponential distributions (68b), $\Delta = \exp\{-\pi[1 + (2t_c)^{-1}]\}$ is always less than its $\beta_c \rightarrow 0$ limit $\Delta_0 = \exp(-3\pi/2) = 9 \times 10^{-3}$. For uniform distributions (68a), this upper bound reads $\Delta_0 = 1 \times 10^{-11}$.

Figure 6 shows plots of the free energy amplitude $R(\beta - \beta_c)$ defined in Eq. (71). Our numerical data have been obtained as follows. We have replaced the transfer operators T_n by finite-dimensional matrices ($0 \leq h \leq h_{\max}$), computed the Ω_N recursively, extracted the free energy from Eq. (70), and averaged the results over a large number of values of N lying between $N_{\max}/2$ and N_{\max} . In order to have data with reasonable error bars, i.e., comparable to the symbol size on Fig. 6, a very large number of iterations was needed (N_{\max} going from 10^6 to 10^7 , as $\beta - \beta_c$ ranges from 0.2 to 0.02). We shall comment on the influence of the matrix truncation size h_{\max} later, when we present data for the mean height w . Our data for the uniform and exponential substrate potential distributions are presented on the same Fig. 6, together with the exact result (solid line) corresponding to the annealed model having the same β_c . The parameters u_1, u_2 of the distributions have been chosen in such a way that $t_c = \exp(-\beta_c) = 0.6$ in both cases. The lines going through both series of points are just least-

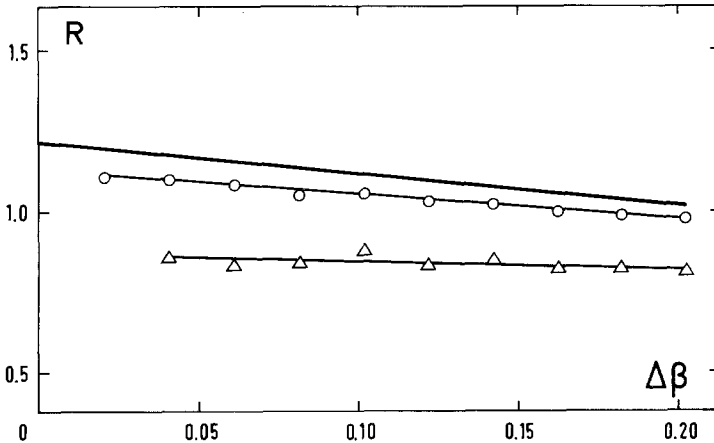


Fig. 6. Plot of the amplitude R of the free energy difference between the localized and extended phases, defined in Eq. (71), versus $\Delta\beta \equiv \beta - \beta_c$, showing numerical data for (Δ) the exponential and (\circ) uniform substrate potential distributions. The thick line represents the exact result for the effective annealed model having the same critical temperature ($t_c = 0.6$) as both random systems. The thin lines (least-squares fits) are guides to the eye.

squares linear fits, mainly thought of as guides for the eye. Just as could be expected from our estimate (73) of the size of the critical region, the logarithmic corrections (72b) to the specific heat jump are *invisible* at the values of $\beta - \beta_c$ that can be reached by our numerical scheme.

We now turn to the mean interface height defined through

$$w = \lim_{N \rightarrow 0} \left(N^{-1} \sum_{n=1}^N \|\Omega_n\|_1^{-1} (\Omega_n)_h \right) \quad (74)$$

where the norm of Ω_n reads as in Eq. (70b). This quantity is averaged with respect to both the thermal fluctuations of the interface and the substrate potential distribution. It has been shown in Section 7 that the mean height diverges, as the critical temperature is reached from below, just as in the pure model

$$w \sim A(\beta - \beta_c)^{-1} \quad (75)$$

where A is a model-dependent constant. No logarithmic correction is expected to modify this simple power-law critical behavior.

Figure 7 shows plots of the amplitude

$$P(\beta - \beta_c) = (\beta - \beta_c)w \quad (76)$$

This product hence approaches a finite value $P(0) \equiv A$ as β goes to β_c . The numerical values of P have been extracted from the very same long sequences of state vector Ω_N that were used to determine the free energy. The data

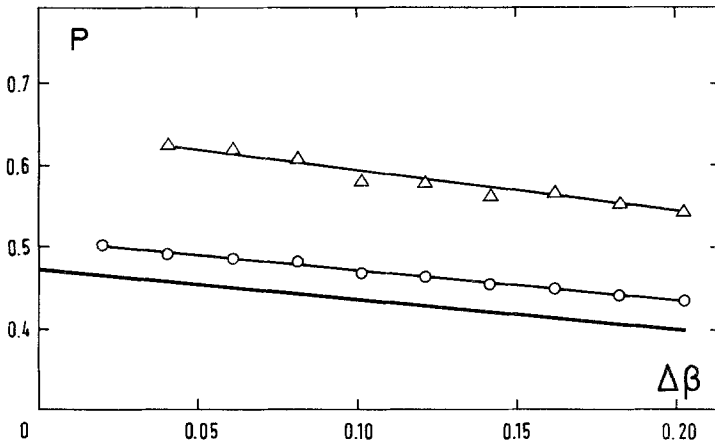


Fig. 7. Same as Fig. 6, for the amplitude P of the mean interface height w , defined in Eq. (76).

are reliable as long as the truncation size h_{\max} is much larger than the mean height w . It has been sufficient to take $h_{\max} = 500$ for $\beta - \beta_c \geq 0.02$ in the case under consideration. The data corresponding to the uniform and exponential potential distributions are again presented on the same Fig. 7, together with the exact annealed result, and the thin lines still represent least-squares fits.

These numerical results show that two essential physical quantities of the critical wetting of a disordered substrate in two dimensions, namely the free energy and the mean interface height, are numerically very close to their values in the equivalent annealed model introduced in Section 2, and hence are not very sensible to substrate randomness, except in a *very* small critical region, where disorder generates logarithmic deviations to the power laws of the pure system.

9. GENERALIZATION AND CONCLUSIONS

Let us now discuss some aspects of the low-temperature limit of the model.

For temperatures going to zero, entropy effects can be neglected, and the interface will in principle be straight. If the wall potential is purely attractive, the interface will be at the wall ($h_i = 0$) at $T = 0$. Excitations will have Boltzmann factors $e^{-2\beta J}$, indicating that one step away from the wall and one step back to it have to be made.

If the wall potential has repelling parts, the problem becomes more interesting. Then the interface may avoid regions with large repulsion by going one step away from the wall ($h_i = 1$ for $i_0 \leq i \leq i_1$). Whenever the energy cost $2J$ for making two steps is less than the repulsive energy $(-)\sum_{i=i_0}^{i_1} u_i$, the interface will make such a wandering.

The picture of only considering states with $h_i = 0$ or $h_i = 1$ is just that of an Ising chain in a random magnetic field. Writing $h_i = \frac{1}{2}(1 - s_i)$, with $s_i = \pm 1$, the corresponding spin Hamiltonian is

$$H = -\frac{1}{2}J \sum_{i=1}^N S_i S_{i+1} - \frac{1}{2} \sum_{i=1}^N u_i S_i + \frac{1}{2}NJ - \frac{1}{2} \sum_{i=1}^N u_i \quad (77)$$

This problem is known to have an interesting low-temperature behavior if frustration is present, that is, if both attracting ($u_i > 0$) and repelling ($u_i < 0$) wall potentials or random magnetic fields occur. Here we summarize some of the known results.

One can define probabilities $P_n(h)$ that the interface takes the value h after n steps in terms of the transfer matrices T_i ,

$$P_n(h) = (T_n T_{n-1} \cdots T_1)_{h,0} \left/ \sum_{h'=0}^{\infty} (T_n \cdots T_1)_{h',0} \right. \quad (78)$$

with

$$(T_k)_{h,h'} = \exp(-\beta J|h-h'| + \beta u_k \delta_{h',0}) \tag{79}$$

and from this the local wall potential v_n by

$$e^{-\beta V_n} = P_n(1)/P_n(0) \tag{80}$$

In the pure case, one has $v_n = T\mu$, with μ defined by Eq. (19). At $T=0$ this reduces to $v = u + J$, indicating the cost of kink and attraction energy.

At the phase transition ($\mu = 0$), there is essentially no attraction by the wall, and indeed the interface wanders infinitely far away.

If the wall potentials u_n have a random distribution, so do the v_n . The binary case $u_n = \pm u$ was studied by several authors. Bruinsma and Aeppli⁽¹⁴⁾ showed that, in the $n \rightarrow \infty$ limit, the local wall potential v_n may take values on a Cantor set, its distribution function being a complete devil's staircase. Derrida *et al.*⁽¹⁵⁾ calculated the ground-state energy and entropy. These quantities are discontinuous whenever the condition $2J = nu$ is satisfied for some integer n . This can be understood as follows. Suppose that one has a region in the system with $u_i = -u$ for $i_0 + 1 \leq i \leq i_0 + n$ and that the outer parts $i \leq i_0$ and $i \geq i_0 + n + 1$ favor the situation where $h_{i_0} = h_{i_0+n+1} = 0$. Then the state with $h_i = 0$ for $i_0 + 1 \leq i \leq i_0 + n$ has an energy contribution equal to $+nu$, whereas the state with $h_i = 1$ for $i_0 + 1 \leq i \leq i_0 + n$ has an energy contribution equal to $2J$. When $2J = nu$, both states are degenerate. This effect gives rise to discontinuities in several physical quantities.

Another interesting case is the large coupling limit ($J \gg 1$). We have already mentioned the mechanism of going one step away from the wall, in order to escape from regions with large repulsion. Derrida and Hilhorst⁽¹⁶⁾ have shown that the leading behavior of the free energy in the $J \rightarrow \infty$ limit reads

$$-\beta f = \bar{u} + Ae^{-2\alpha^*J} + Ce^{-2\beta J} \tag{81}$$

where the exponent α^* is the absolute value of the nonzero, real solution

$$\int \rho(u) du e^{-\alpha u} = 1 \tag{82}$$

Indeed, if all the u 's are positive (only attraction), such a solution does not exist. If there is also repulsion, α^* does exist, and for $\beta > \alpha^*$ the second term in (81) is the leading correction.

Exact solutions of the random field Ising chain at all temperatures were discussed by Nieuwenhuizen and Luck.⁽¹⁷⁾ These authors consider diluted symmetric and diluted asymmetric exponential distributions. In the

first case, there is always a positive ground-state entropy; in the second case, this is so only for resonance conditions, as in the binary case discussed above. The specific heat was found to be linear in T for small T . Numerical factors, such as the $T=0$ energy, entropy, the specific heat amplitude, and the amplitude A of the strong coupling behavior (81), could be expressed in terms of coefficients related to the (complex) solutions of Eq. (82).

Another quantity of interest is the two-spin correlation function of such Ising-like systems. Grinstein and Mukamel⁽¹⁸⁾ have considered a system with strong pinning ($u_i=0$ or $u_i > +2J$ or $u_i < -2J$). Then the interface is pinned at $h_i=0$ if $u_i > +2J$ and at $h_i=1$ if $u_i < -2J$, whereas it may be at $h_i=0$ or $h_i=1$ at sites where $u_i=0$. It was found that the two-point function has a Lorentzian + Lorentzian-squared shape.

Finally, let us discuss the symmetric model, where the interface can be pinned on a line *in the bulk*. The Hamiltonian of the RSOS model for this system is still given by (1), but now the height variables h_i take all positive and negative integer values. It is easy to show that the interface in this model will always be pinned at $T=0$, as soon as some attraction is present ($u_i > 0$). For large temperatures, on the other hand, the interface will wander away if the potential is repelling on the average ($\bar{u} < 0$), as we now show. In contrast to the model with a wall, there is no loss of entropy in the present case, so that only the energy need be considered. In particular, if the potential is attractive on the average, the interface will be pinned at all finite temperatures.

The symmetric model has a transfer matrix

$$\begin{aligned} T_n(h, h') &= \delta_{hh'} + t\delta_{h, h'+1} + t\delta_{h, h'-1} & (h \neq 0) \\ &= y_n(\delta_{0, h'} + t\delta_{1, h'} + t\delta_{-1, h'}) & (h = 0) \end{aligned} \quad (83)$$

By the transformation

$$\begin{aligned} S_{hh'} &= (1/\sqrt{2})(-\delta_{hh'} + \delta_{h, -h'}) & (h < 0) \\ &= (1/\sqrt{2})(\delta_{hh'} + \delta_{h, -h'}) & (h > 0) \\ &= (1/\sqrt{2})\delta_{h, h'} & (h = 0) \end{aligned} \quad (84)$$

it can be mapped onto

$$\tilde{T}_n = S^{-1}T_nS = \begin{pmatrix} \tilde{T}_- & 0 \\ 0 & \tilde{T}_{n+} \end{pmatrix}$$

with

$$\begin{aligned}
 \tilde{T}_{-,hh'} &= \delta_{h,h'} + t(\delta_{h,h'+1} + \delta_{h,h'-1}) & (h < -2) \\
 &= \delta_{h,h'} + t\delta_{h,h'-1} & (h = -1) \\
 &= 0 & (h, h' \geq 0) \\
 \tilde{T}_{n+,hh'} &= \delta_{h,h'} + t(\delta_{h,h'+1} + \delta_{h,h'-1}) & (h \geq 1) \\
 &= y_n(\delta_{h,h'} + 2t\delta_{h,h'-1}) & (h = 0) \\
 &= 0 & (h, h' \leq 0)
 \end{aligned} \tag{85}$$

Since the upper matrix \tilde{T}_- decouples, it can be omitted from the calculations of the free energy. The only change with respect to the situation with a wall is that the $(0, 1)$ element of \tilde{T}_{n+} has an additional factor of 2.

In the ordered situation, $y_n = y$, T_n has a localized state $\psi(h) \sim e^{-\mu|h|}$, and \tilde{T}_{n+} a related state $e^{-\mu h}$ ($h \geq 0$), with μ defined by [compare with (19)]

$$y(1 + 2te^{-\mu}) = 1 + 2t \cosh \mu \tag{86}$$

Indeed, the critical point ($\mu = 0$) is at the value $y \equiv e^{\beta u} = 1$, where the potential u changes from attracting to repelling. According to the results of the preceding sections, in random systems, the critical point is given by

$$\int \rho(u) e^{\beta_c u} du = 1 \tag{87}$$

This equation has a solution with a finite T_c whenever both attracting and repelling values of u occur, but on the average the line is repelling ($\bar{u} < 0$).

In conclusion, we have shown that wetting of a disordered substrate in 2d is very similar to that of a pure system. Disorder along a line (substrate) is not sufficient to change the universal properties of the wetting transition. Its effect shows up as logarithmic corrections to the free energy and specific heat. If the disorder is along a line in the bulk, (symmetric model), then there is no depinning transition in the pure case if u , the pinning potential, is attractive. On the other hand, in the presence of disorder, with $\bar{u} < 0$, a depinning transition at finite temperature does take place.

The above results are exact; they have been obtained by an infinite resummation of a field-theoretic perturbation series in terms of Goldstone diagrams. The only questionable point, namely the validity of the replica trick, has been verified numerically.

Although the actual calculations have been performed for an RSOS model, the same conclusions hold for Abraham's Ising model version of 2d wetting.⁽⁶⁾

ACKNOWLEDGMENT

One of us (J. M. L.) wishes to thank Dr. U. Glaus for stimulating discussion concerning numerical work on related models.

REFERENCES

1. P. G. de Gennes, *Rev. Mod. Phys.* **57**:827 (1985); M. E. Fisher, in *Fundamental Problems in Statistical Mechanics VI* (North-Holland, Amsterdam 1985); E. H. Hauge, in *Fundamental Problems in Statistical Mechanics VI*; D. Sullivan and M. M. Telo de Gama, in *Fluid Interfacial Phenomena*, C. A. Craxton, ed. (Wiley, New York, 1985).
2. G. Forgacs, H. Orland, and M. Schick, *Phys. Rev. B* **32**:4683 (1985).
3. M. Kardar, *Phys. Rev. Lett.* **55**:2235 (1985).
4. R. Lipowsky and M. E. Fisher, *Phys. Rev. Lett.* **56**:472 (1986).
5. A. B. Harris, *J. Phys. C* **7**:1671 (1974).
6. D. Abraham, *Phys. Rev. Lett.* **44**:1165 (1980).
7. J. M. J. van Leeuwen and H. J. Hilhorst, *Physica* **107A**:319 (1981); S. T. Chui and J. D. Weeks, *Phys. Rev. B* **23**:2438 (1981).
8. J. Goldstone, *Proc. R. Soc.* **239A**:267 (1957).
9. B. D. Day, *Rev. Mod. Phys.* **39**:719 (1957).
10. B. H. Brandow, *Rev. Mod. Phys.* **39**:771 (1957).
11. G. Forgacs, J. M. Luck, Th. M. Nieuwenhuizen, and H. Orland, *Phys. Rev. Lett.* **57**:2184 (1986).
12. G. Gentile, *Nuovo Cimento* **17**:493 (1940); **19**:109 (1942); G. Schubert, *Z. Naturforsch.* **1**:113 (1946); B. H. Brandow, *Ann. Phys. (N.Y.)* **64**:21 (1971).
13. D. J. Amit, in *Field Theory, Critical Phenomena and the Renormalization Group* (McGraw-Hill, 1978).
14. R. Bruinsma and G. Aeppli, *Phys. Rev. Lett.* **50**:1494 (1983).
15. B. Derrida, J. Vannimenus, and Y. Pomeau, *J. Phys. C* **11**:4749 (1978).
16. B. Derrida and H. J. Hilhorst, *J. Phys. A* **16**:2641 (1983).
17. Th. M. Nieuwenhuizen and J. M. Luck, *J. Phys. A* **19**:1207 (1983).
18. G. Grinstein and D. Mukamel, *Phys. Rev. B* **27**:4503 (1983).